

Extraction of urban vegetation with Pléiades multi-angular images

Antoine Lefebvre^a, Jean Nabucet^b, Thomas Corpetti^b, Nicolas Courty^a, and Laurence Hubert-Moy^c

^aCNES, UMR 6074 IRISA, Campus de Tohannic, Vannes, France

^bCNRS, UMR 6552 LETG, Place du recteur Henri Le Moal, Rennes, France

^cUniversité Rennes 2, UMR 6552 LETG, Place du recteur Henri Le Moal, Rennes, France

ABSTRACT

Vegetation is essential in urban environments since it provides significant services in terms of health, heat, property value, ecology ... As part of the European Union Biodiversity Strategy Plan for 2020, the protection and development of green-infrastructures is strengthened in urban areas. In order to evaluate and monitor the quality of the green infra-structures, this article investigates contributions of Pléiades multi-angular images to extract and characterize low and high urban vegetation. From such images one can extract both spectral and elevation information from optical images. Our method is composed of 3 main steps : (1) the computation of a normalized Digital Surface Model from the multi-angular images ; (2) Extraction of spectral and contextual features ; (3) a classification of vegetation classes (tree and grass) performed with a random forest classifier. Results performed in the city of Rennes in France show the ability of multi-angular images to extract DEM in urban area despite building height. It also highlights its importance and its complementarity with contextual information to extract urban vegetation.

Keywords: Urban vegetation, Multi-angular images, Digital elevation model, Remote sensing

1. INTRODUCTION

Green frames and green-infrastructures are obviously credible answers to new challenges that cities have to face. Vegetation has now an important part in all recent urban plans. It has indeed been demonstrated that green areas provide numerous ecological services such as biodiversity conservation,¹ heat island and air pollution reduction.² It has also been highlighted that they contribute to human well-being³ and increase value of neighbored real estate.⁴ However urban vegetation is difficult to monitor and manage and local decision makers are still looking for an effective assesment of its functionalities. Indeed, the databases on urban vegetation are still limited and are primarily made from field mission. At the European scale for example, the Copernicus land services took the initiative to map urban vegetation for cities of more than 50,000 residents. However the minimal mapping unit is fixed to 500m² patch whose width is greater than 10m.⁵ This data cannot be used to extract individual trees or small hedges network. Such small vegetated objects are visible on Very High Resolution (VHR) images with sub-metric spatial resolution and their automatic extraction processing has already been presented in numerous papers.⁶⁻⁹ These studies mainly focus on the contribution of the spectral and texture information of VHR images. However, few papers have evaluated the capabilities of some platforms, such as Pléiades, to generate Digital Elevation Model from multi-angular images and their contributions to extract urban vegetation.

This article investigates contributions of Pléiades multi-angular images to extract and characterize low and high urban vegetation. It is proposed to produce a normalized DSM (nDSM) and to combine it successively to well-know spectral and contextual features.

Further author information: (Send correspondence to Antoine Lefebvre)
E-mail: lefebvre.antoine@gmail.com, +33 (0)2 99 14 18 47

2. MATERIALS AND METHODS

2.1 Study area and data

The study area is the city of Rennes in France. It is a mid-sized city of about 2,500km² with over 200,000 inhabitants. The study focuses on 4 different urban landscapes (Fig.1) : public garden in the city center, university campus, urban housing, suburban housing. This dataset was selected to reflect the heterogeneity of the urban landscape. For example, the city center embeds small and connected buildings whereas university campus is composed of large, individual and high buildings. As a consequence the vegetation organization is also different and suburban housing is mainly composed of private backyard while city center includes more public tree lines along the roads.

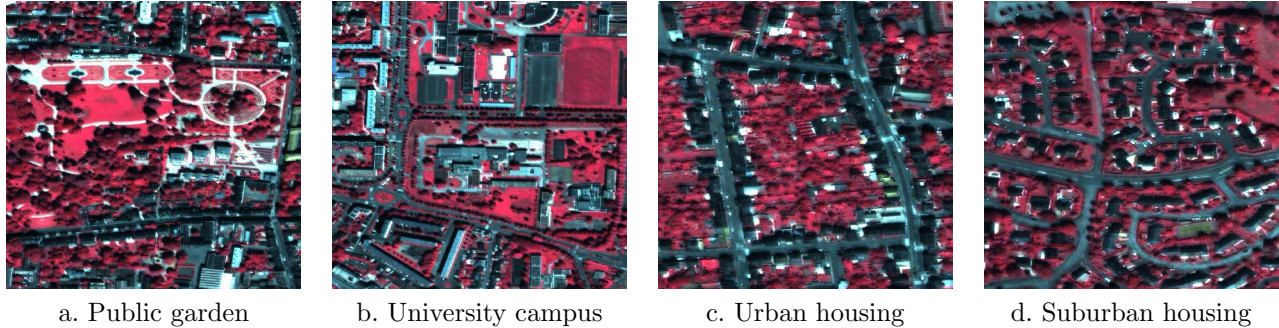


FIGURE 1. Presentation of the 4 urban landscapes with combination Pléiades pan-sharpened bands (Green, Red, Near-infrared).

The available data is a pair of Pléiades images acquired with PHR-1A platform at the 14th August 2013 at AM 11 :10 :57 and AM 11 :11 :12. The incidence angles are presented in table 1. It can be notice that we gave preference to low incidence angles to limit hidden surfaces by building frontages.

TABLE 1. Acquisition parameters of Pléiades data.

Name	Time	Incidence Angles (degree)		
		Along Track	Across Track	Overall
Image 1	AM 11 :10 :57	-3.403	6.713	7.512
Image 2	AM 11 :11 :12	5.492	4.528	7.100

2.2 Features computation

2.2.1 Normalized Digital Surface Model

Among the numerous softwares and approaches to generate a DSM from Pléiades images,^{10,11} the ERDAS eATE software was selected for its automatic processing and its reliability to process large scene. The elevation information was computed with the panchromatic band of the Pléiades images.

To obtain a uniform information about height of urban objects (building, trees ..), it is necessary to create a DSM that compensate the bare earth relief. The Normalized Digital Surface Model (nDSM) is then the subtraction of the DSM and the Digital Elevation Model (DEM). To this end, generation of the DEM consists in removing all objects (buildings, trees, bridges...) from DEM. This step was performed with slope based algorithm.¹² This method assumes that a large height difference (slope) between two nearby pixels is due to an object and can then be removed. Fig. 2 provides an example of the result obtained.

2.2.2 Features based on spectral bands

All multispectral bands (blue, green, red, near-infrared) were used for classification. A pansharpening with panchromatic band was performed with the subtractive resolution merge method, which is relatively radiometrically accurate.¹³

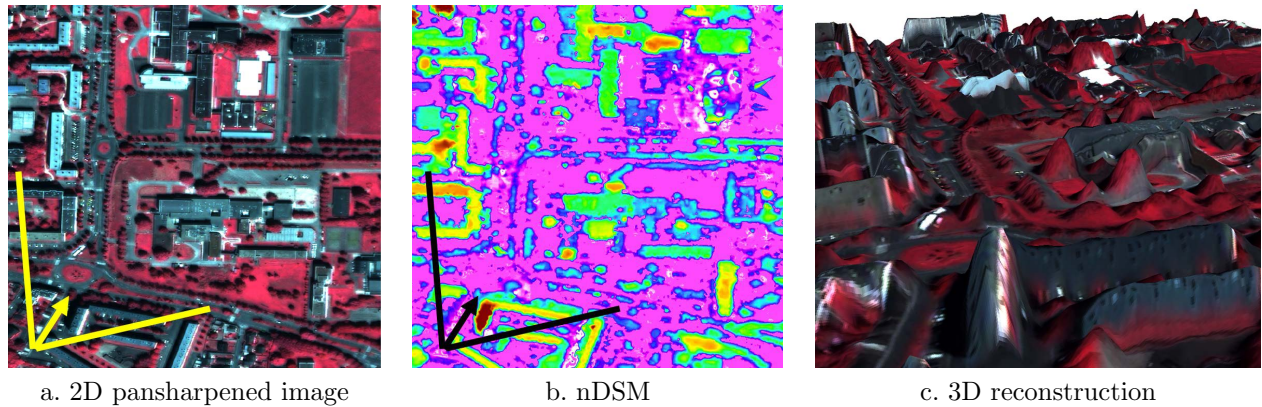


FIGURE 2. Example of nDSM obtained with ERDAS eATE and slope based smoothing on the University Campus study site.

In addition, the Normalized Difference Vegetation Index was used (Eq 1).

$$NDVI = \frac{R - NIR}{R + NIR}, \quad (1)$$

where R is the red band and NIR the near-infrared. It is an essential information to extract vegetation and it is also suitable to limit shadow effects.¹⁴

We also add the Normalized Difference Water Index (NDWI) is also used (Eq 2).

$$NDWI = \frac{G - NIR}{G + NIR}, \quad (2)$$

where G is the green band and NIR the near-infrared. In contrary to the $NDVI$, this metric is usually used to extract dark object such as water and shadow.¹⁵

2.2.3 Contextual features

A precise characterization and description of urban trees is a complex task. Trees can indeed be isolated, organized as a line or grouped in patch. They can also be cut thinly or not. The multispectral information is often insufficient and contextual features providing information on their shape, size and their organization is mandatory. Thus, we selected contextual features based on texture analysis and granulometry.

Among the numerous texture analysis technique, we used the **Grey Level Co-occurrence Matrix (GLCM)** because of their efficiency in numerous characterization of remote sensing data.¹⁶ Any GLCM is associated with a direction \mathbf{u} . For a given pattern $I(\mathbf{x})$ (with $\mathbf{x} = (x, y)$ the spatial coordinates), the approach consists in computing a matrix $G_{\mathbf{u}}$ of size $N \times N$ (with N the number of grey-levels) where each element $g(i, j) = G_{\mathbf{u}}(i, j)$ is the number of pairs of pixels such that $I(\mathbf{x}) = i$ and $I(\mathbf{x} + \mathbf{u}) = j$. Several criteria can then be computed from $G_{\mathbf{u}}$ to describe a texture pattern. Among them, we selected the contrast, the energy and the entropy respectively defined in eq. (3), (4) and (5) where $g(i, j)$ corresponds to the element (i, j) in matrix $G_{\mathbf{u}}$:

$$Contrast = \sum_{i,j} (i - j)^2 \cdot g(i, j), \quad (3)$$

$$Energy = \sum_{i,j} g(i, j)^2, \quad (4)$$

$$Entropy = - \sum_{i,j} g(i, j) \ln g(i, j). \quad (5)$$

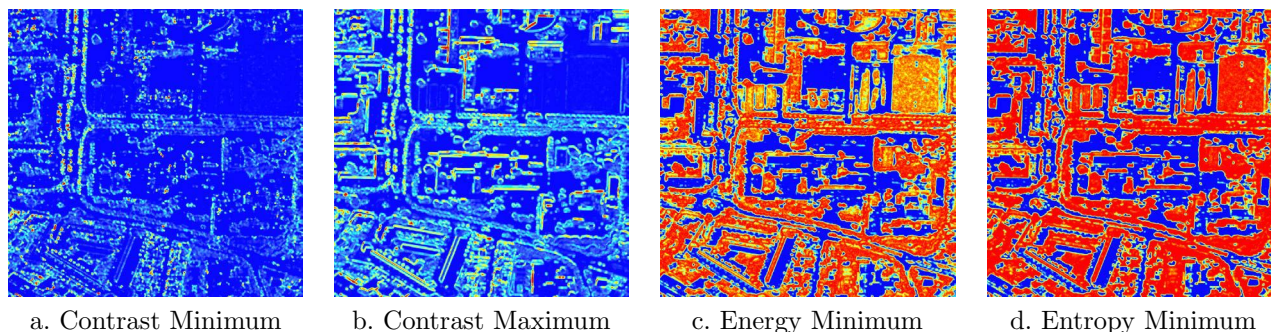


FIGURE 3. Example of texture features compute on the University Campus study site.

However, these features provide information in a given direction \mathbf{u} and are then rotation sensitive.¹⁷ To be rotation invariant, the descriptors are computed in 10 different directions and the minimum and maximum value are kept,^{16,18} as shown in Fig. 3.

In addition to GLCM, we compute the **granulometry** which is based on successive openings (and closings) by reconstruction with structuring elements (SE) of various size.¹⁹ We first compute Morphological Profile (*MP*), defined for a level ℓ as :

$$MP_{\ell}^R(x) = \phi_{\ell}^R(I(x)) \quad (6)$$

where x is a pixel of the image I and ϕ_{ℓ}^R , with $R = \{o, c\}$, is the operation of opening ($R = o$) or closure ($R = c$) using a structural element of size ℓ . Such *MP* provide both spatial and radiometric information and are very interesting for the contextual description of the image.²⁰ A derived version, Differential Morphological Profiles (*DMP*), consists in the subtraction of *MP* for various scales of structuring elements :

$$DMP_i^R(x) = MP_{\mathcal{N}(i+1)}^R(x) - MP_{\mathcal{N}(i)}^R(x) \quad (7)$$

where \mathcal{N} is a set of growing scales of SE (in practice we use $\mathcal{N} = \{3, 7, 11, 15, 19\}$). The *DMP* have shown their performance to extract green linear elements^{21,22} and also urban environment.²³ As can be shown in Fig. 4, *DMP* are very interesting since isolated trees appear in the first component and the large tree lines in the third or fourth component.

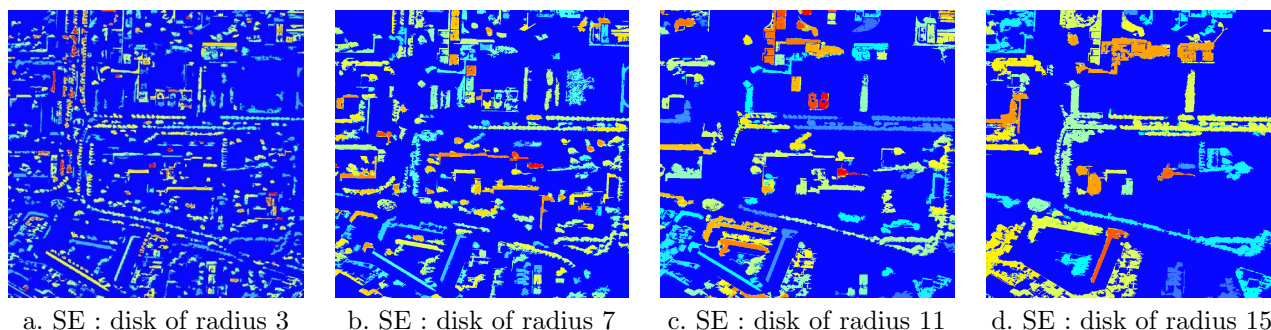


FIGURE 4. Example of *DMP* on the University Campus of Rennes, France.

2.3 Classification of urban vegetation

GLCM and granulometry based on *DMP* are then used to describe green areas in cities. As for the classification, the training dataset is composed of 6 thematic classes : Low vegetation (grass), High vegetation (tree), Road network and Building. Samples was manually edited homogeneously on the Pléiades pan-sharpened images on overall city. Classification was performed with the bagging trees algorithm which is part of ensemble methods such as random forest and boosting.²⁴ Ensemble methods are suitable to classify remote sensing image in urban areas^{9,16} and is less sensitive to irrelevant features (in contrast to SVM or neural networks).

2.4 Ground truth for validation

Two validation datasets were used. Both were edited manually on the Pléiades pan-sharpened images. However, samples were selected inside the extent of the 4 urban landscapes (presented in sec 2.1).

The first dataset consists in the selection of three thematic classes (Low vegetation, High vegetation, Mineral objects) and is used to validate the overall accuracy of the classification. The second validation dataset has been defined in order to understand the effect of the urban landscape on the misclassification of high vegetation. Five thematic was selected : Isolated tree ($> 10\text{m}$), Isolated tree ($< 10\text{m}$), Tree lines ($> 10\text{m}$), Tree lines ($< 10\text{m}$), Tree patch.

3. RESULTS AND DISCUSSION

A set of 4 classifications with different features combination was performed to evaluate the contribution of the elevation information :

1. Spectral features (MS)
2. Spectral features + nDSM ($MS + DSM$)
3. Spectral features + Contextual features ($MS + CON$)
4. Spectral features + Contextual features + nDSM ($MS + CON + DSM$).

The classifications on the 4 urban landscapes are presented in Fig. 3 and their associated Kappa index in Fig. 6. A significant difference can be noticed between MS and other classifications. The $nDSM$ improves the Kappa index by 0.82 to 0.89 for all classifications. However this difference is less important compared to $MS + CON$ classifications. This highlights the importance of contextual features to extract urban vegetation. The $nDSM$ also improves the classification and allows to increase Kappa index by 0.94 to 0.95.

Visually, the results are consistent with the statistical analysis. MS classifications (first column of figure 5) include a salt and pepper noise and the $MS + CON$ classifications seem to provide a coarser result including more commission errors for the tree class. It can be observed that some landscapes are easier to analyze than others. For example, the Public Garden is composed of large compact surfaces of vegetation. Conversely, the urban and suburban residential areas have a large number of private land where low vegetation and high are heterogeneous and mixed. In these cases, the $nDSM$ and contextual information is essential.

The Fig. 7 shows the rate of commission and omission errors for the tree class. The error rate decreases with the addition of features. While one might think that $MS + CON$ and $MS + CON + DSM$ classifications are similar, results show that $MS + CON + DSM$ classifications have the advantage to reduce significantly the commission errors. This result confirms the visual interpretation presented previously.

Finally, we analyzed the omission errors for the tree class. It can be noticed that classifications including $nDSM$ tends to omit small items such as tree lines ($< 10\text{m}$) and single trees ($< 10\text{m}$). Its combination with contextual information is thus complementary. It detects smaller objects while limiting commission errors.

4. CONCLUSION

This article focuses on the extraction of urban vegetation from Pléiades multi-angular images. We evaluated the contribution of the $nDSM$ built with stereo-pair images to extract urban vegetation. Several sets of features were computed and evaluated on different urban landscapes with the bagging tree algorithm. Results reveal that stereo-pair images improve the extraction of vegetation whatever the cityscape. We also demonstrated that contextual information (texture, granulometry) is complementary with elevation information. It allows to extract small objects such as isolated trees or fine alignments and limit commission errors. Future works should attempt to classify different vegetation classes and evaluate its contribution at the city scale to meet the needs of national and European policy makers.

5. ACKNOWLEDGMENT

Authors gratefully acknowledge the support of the CNES TOSCA VEGIDAR project and CNES Kalideos Bretagne program, without which the present study could not have been completed

REFERENCES

- [1] Croci, S., Butet, A., Georges, A., Aguejdad, R., and Clergeau, P., "Small urban woodlands as biodiversity conservation hot-spot : a multi-taxon approach," *Landscape Ecology* **23**, 1171–1186 (aug 2008).
- [2] Nowak, D. J., Crane, D. E., and Stevens, J. C., "Air pollution removal by urban trees and shrubs in the United States," *Urban Forestry & Urban Greening* **4**, 115–123 (apr 2006).
- [3] Weber, C. and Hirsch, J., "Some urban measurements from SPOT data : urban life quality indices," *International Journal of Remote Sensing* **13**, 3251–3261 (nov 1992).
- [4] Dwyer, J. F., Mcpherson, E. G., Schroeder, H. W., and Rowntree, R. A., "Assessing the benefits and costs of the urban forest," *Journal of Arboriculture* **18**(5), 227–234 (1992).
- [5] Lefebvre, A. and Sannier, C., "Mapping tree cover in European cities : comparison of classification algorithms for an operational production framework," in [*Joint Urban Remote sensing Event (JURSE 2015)*], (2015).
- [6] Carleer, A. P. and Wolff, E., "Urban land cover multi-level region-based classification of VHR data by selecting relevant features," *International Journal of Remote Sensing* **27**, 1035–1051 (mar 2006).
- [7] Nichol, J. and Lee, C. M., "Urban vegetation monitoring in Hong Kong using high resolution multispectral images," *International Journal of Remote Sensing* **26**, 903–918 (mar 2005).
- [8] Pu, R. and Landry, S., "A comparative analysis of high spatial resolution IKONOS and WorldView-2 imagery for mapping urban tree species," *Remote Sensing of Environment* **124**, 516–533 (sep 2012).
- [9] Puissant, A., Rougier, S., and Stumpf, A., "Object-oriented mapping of urban trees using Random Forest classifiers," *International Journal of Applied Earth Observation and Geoinformation* **26**, 235–245 (feb 2014).
- [10] Durand, A., Michel, J., De Franchis, C., Allenbach, B., and Giros, A., "Qualitative assessment of four DSM generation approaches using Pléiades-HR data," *Proceedings of the 33th . . .* (2013).
- [11] Perko, R., Raggam, H., Gutjahr, K., and Schardt, M., "Assessment of the mapping potential of Pléiades stereo and triplet data," *ISPRS Annals of Photogrammetry, Remote Sensing and Spatial Information Sciences* **II-3**(September), 103–109 (2014).
- [12] Vosselman, G., "Slope based filtering of laser altimetry data," *International Archives of Photogrammetry and Remote Sensing, Vol. 33, Part B3/2* **33**(Part B3/2), 678–684 (2000).
- [13] Aguilar, M. a., Saldana, M. M., and Aguilar, F. J., "GeoEye-1 and WorldView-2 pan-sharpened imagery for object-based classification in urban environments," *International Journal of Remote Sensing* **34**(7), 2583–2606 (2013).
- [14] Zhang, L., Sun, X., Wu, T., and Zhang, H., "An Analysis of Shadow Effects on Spectral Vegetation Indexes Using a Ground-Based Imaging Spectrometer," *IEEE Geoscience and Remote Sensing Letters* **12**(11), 2188–2192 (2015).
- [15] Salehi, B., Zhang, Y., Zhong, M., and Dey, V., "Object-based classification of urban areas using VHR imagery and height points ancillary data," *Remote Sensing* **4**(8), 2256–2276 (2012).
- [16] Lefebvre, A., Sannier, C., and Corpetti, T., "Monitoring Urban Areas with Sentinel-2A Data : Application to the Update of the Copernicus High Resolution Layer Imperviousness Degree," *Remote Sensing* **8**(7), 606 (2016).
- [17] Lefebvre, A., Corpetti, T., and Hubert-Moy, L., "Estimation of the orientation of textured patterns via wavelet analysis," *Pattern Recognition Letters* **32**, 190–196 (oct 2011).
- [18] Pesaresi, M., Gerhardinger, A., and Kayitakire, F., "A Robust Built-Up Area Presence Index by Anisotropic Rotation-Invariant Textural Measure," *IEEE Journal of Selected Topics in Applied Earth Observations and Remote Sensing* **1**, 180–192 (sep 2008).
- [19] Fauvel, M., *Spectral and Spatial Methods for the Classification of Urban Remote Sensing Data*, PhD thesis, Grenoble Institute of Technology ; Faculty of Engineering - University of Iceland (2007).
- [20] Pesaresi, M. and Benediktsson, J. A., "A new approach for the morphological segmentation of high-resolution satellite imagery," *IEEE Transactions on Geoscience and Remote Sensing* **39**, 309–320 (2001).
- [21] Aksoy, S., Akcay, H., and Wassenaar, T., "Automatic Mapping of Linear Woody Vegetation Features in Agricultural Landscapes Using Very High Resolution Imagery," *IEEE Transactions on Geoscience and Remote Sensing* **48**, 511–522 (jan 2010).
- [22] Fauvel, M., Arbelot, B., Benediktsson, J. A., Sheeren, D., and Chanussot, J., "Detection of Hedges in a Rural Landscape Using a Local Orientation Feature : From Linear Opening to Path Opening," *IEEE Journal of Selected Topics in Applied Earth Observations and Remote Sensing* **6**, 15–26 (feb 2013).
- [23] Chanussot, J., Benediktsson, J. A., and Fauvel, M., "Classification of remote sensing images from urban areas using a fuzzy possibilistic model," *IEEE Geoscience and Remote Sensing Letters* **3**, 40–44 (2006).
- [24] Breiman, L., "Bagging Predictors," *Machine Learning* **24**(421), 123–140 (1996).



FIGURE 5. Classifications on the four urban elements using four combinations of features.

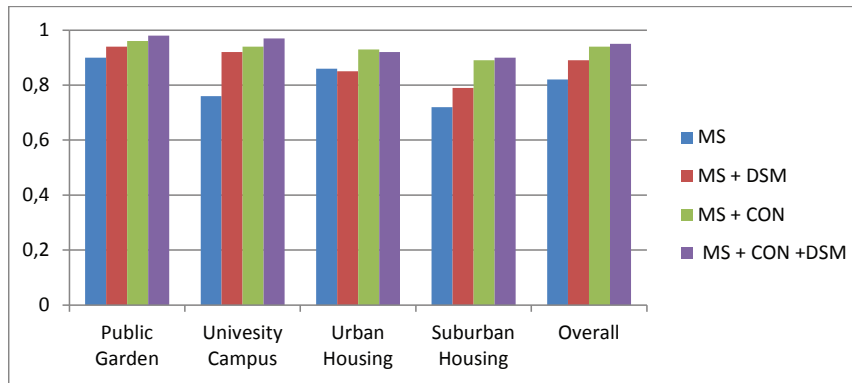


FIGURE 6. Kappa index for the 4 urban landscapes and the overall study site with different features selection.

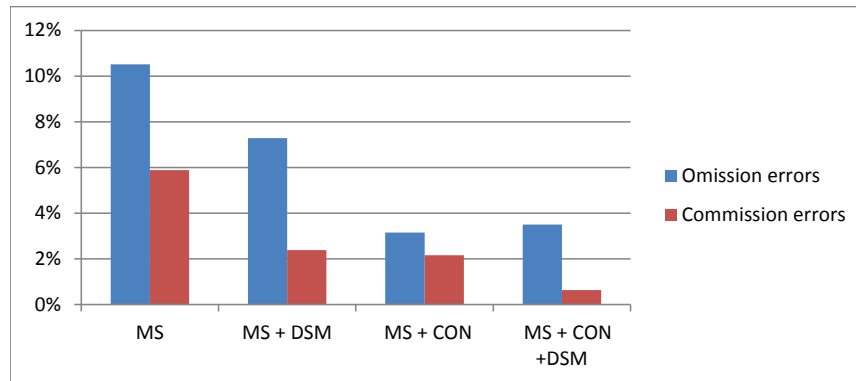


FIGURE 7. Commission and omission errors of high vegetation class for the 4 urban landscapes and the overall study site with different features selection.

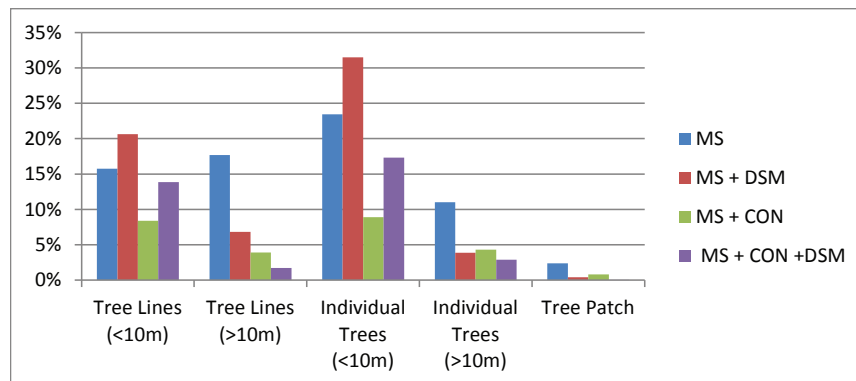


FIGURE 8. Omission errors for 5 high vegetation classes with different features selection.